Pergamon

Int. J. Heat Mass Transfer. Vol. 39, No. 10, pp. 2077–2086, 1996

0017-9310/96 $15.00 + 0.00

0017-9310(95)00298-7

Natural convection from a cylinder with multiple, low-conductivity, longitudinal baffles

G. N. FACAS
Department of Engineering, Trenton State College, Trenton, NJ 08650, U.S.A.

and

H. L. BROWN
Department of Mechanical Engineering and Mechanics, Drexel University, Philadelphia, PA 19104, U.S.A.

(*Received* 12 *January* 1955 *and in final form* 27 *July* 1995)

Abstract—In this paper, the problem of laminar natural convection over an isothermal horizontal cylinder with multiple, low-conductivity, longitudinal baffles is considered. The cylinder is assumed to be suspended in air. Results are obtained numerically over the range $10^3 \leqslant Ra \leqslant 10^6$, $\gamma = 0.25$ and 0.5 and $N = 0$, 1, 3, 5, 11, where γ is the dimensionless baffle length and N is the number of baffles. The results show that baffles are extremely effective in reducing the overall heat loss from the cylinder. Based on the cases considered in this study, energy savings as large as 68.4% (as compared to the case of a cylinder with no-baffles) can be realized if baffles are used. The overall baffle effectiveness increases as the number and baffle length increases. Copyright © 1996 Elsevier Science Ltd.

INTRODUCTION

The problem of laminar natural convection from a horizontal circular cylinder suspended in an infinite fluid medium has been the subject of numerous numerical and experimental investigations [1]. This is due to the importance of this problem from a fundamental, as well as a practical point of view.

The early studies on natural convection over a horizontal isothermal cylinder attempted to predict analytically the local and average Nusselt number. Hermann [2] obtained a solution for the heat transfer from a cylinder by solving the governing boundary-layer equations using the Pohlhausen technique. An integral solution was later presented by Levy [3]. Chiang and Kaye [4] used a Blasius expansion to obtain solutions for horizontal cylinders with varying wall temperature. Empirical relations for the average Nusselt number, which are based on extensive experimental data, have been presented by McAdams [5], Morgan [1], and Churchill and Chu [6].

Kuehn and Goldstein [7] solved the full Navier–Stokes and energy equations for laminar natural convection flow over a horizontal isothermal cylinder using finite differences. Results were presented for the local and average Nusselt number for *Ra* values ranging from 10^0 to 10^7. Their numerical results were in good agreement with available experimental data. Farouk and Guceri [8] considered the problem of natural convection around a circular cylinder with nonuniform surface temperature and heat flux boundary conditions. High accuracy bench mark solutions for natural convection flow around a horizontal circular cylinder with uniform wall temperature were presented by Saitoh *et al.* [9] for *Ra* values in the range 10^3 to 10^5.

Sparrow and Kang [10] considered the problem of natural convection flow over an insulated horizontal circular cylinder. The conjugate conduction–convection problem encompassing the insulation and the fluid exterior to the cylinder was solved numerically using finite differences. Results for the critical radius of insulation were presented as a function of *Ra* and the conductivity ratio k_{ins}/k_{air}.

Jaber *et al.* [11] considered the problem of natural convection flow from a horizontal hot-water pipe embedded within an air-filled, relatively cold rectangular trench. Their measurements indicate that there is an optimal configuration (in terms of the pipe location relative to the cavity walls) which results in the minimum rate of heat loss from the pipe. Neale *et al.* [12] considered the problem of heat transfer from a hot horizontal pipe embedded inside a cold, horizontal rectangular, air-filled duct. The pipe was assumed to be supported by two, low-conductivity, symmetrically-placed spacers/baffles. Their experimental investigation showed that the presence of such spacers could improve the thermal resistance of the air-filled cavity over that of the unobstructed one. An optimal location for the baffles was also identified. Jaber *et al.* [13] investigated experimentally the steady-state heat transfer across a cold, horizontal, rectangular cavity

NOMENCLATURE

D	cylinder diameter
g	gravitational acceleration
Gr	Grashof number
h	local convective coefficient
k	thermal conductivity of fluid
l	baffle length
L	radial distance between cylinder and outer boundary of solution domain
N	number of baffles
Nu	local Nusselt number, hD/k
$\overline{Nu}$	average Nusselt number
R	radial coordinate
r	dimensionless radial coordinate, R/D
Ra	Rayleigh number ($Gr \cdot Pr$)
t	time
T	temperature
T_w	temperature of cylinder surface
T_∞	temperature of ambient fluid
u'	dimensionless radial velocity
v'	dimensionless angular velocity.

Greek symbols

α	thermal diffusivity
β	thermal expansion coefficient
γ	dimensionless baffle length, l/D
θ	angular coordinate, zero is downward vertical
ν	kinematic viscosity
ϕ	dimensionless temperature
τ	dimensionless time
ψ	stream function
ψ'	dimensionless stream function
ω	vorticity
ω'	dimensionless vorticity.

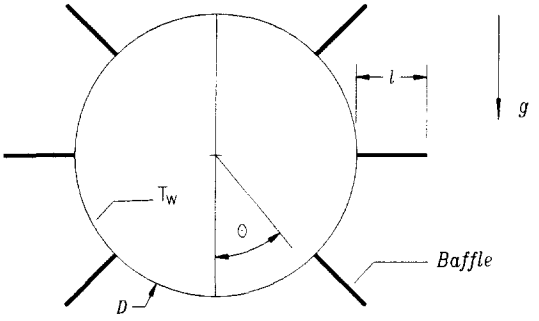

Fig. 1. Geometry and configuration.

enclosing two relatively hot, horizontal pipes. Their results indicate that the minimum steady-state heat loss occurs when the two pipes were placed one above the other. It was also shown that the effective thermal resistance can be further enhanced via the insertion of two pairs of low-conductivity, radial baffles, each supporting one pipe.

The present study deals with natural convection flow over a horizontal cylinder suspended in air with multiple, low-conductivity, longitudinal baffles attached on the external surface of the cylinder, as shown schematically in Fig. 1. The cylinder surface is assumed to be maintained at a constant temperature T_w. Solutions have been obtained numerically over a wide range of Ra values and for two baffle lengths. To the best of our knowledge, this problem has not been solved to date.

MATHEMATICAL FORMULATION

For laminar natural convection flow, the dimensionless Navier–Stokes and energy equation with the Boussinesq approximation may be written in cylindrical coordinates as follows:

$$\nabla^2\psi' = \omega' \tag{1}$$

$$\frac{\partial\omega'}{\partial\tau} + u'\frac{\partial\omega'}{\partial\tau} + \frac{v'}{r}\frac{\partial\omega'}{\partial\theta} = \nabla^2\omega' + Gr\left(\sin\theta\frac{\partial\phi}{\partial r} + \frac{\cos\theta}{r}\frac{\partial\phi}{\partial\theta}\right) \tag{2}$$

$$\frac{\partial\phi}{\partial\tau} + u'\frac{\partial\phi}{\partial r} + \frac{v'}{r}\frac{\partial\phi}{\partial\theta} = \frac{1}{Pr}\nabla^2\phi \tag{3}$$

with

$$\nabla^2 = \frac{\partial^2}{\partial r^2} + \frac{1}{r}\frac{\partial}{\partial r} + \frac{1}{r^2}\frac{\partial^2}{\partial\theta^2} \tag{4}$$

and

$$u' = \frac{1}{r}\frac{\partial\psi'}{\partial\theta} \quad v' = -\frac{\partial\psi'}{\partial r}, \tag{5}$$

where

$$Pr = \frac{\nu}{\alpha} \quad Gr = \frac{g\beta\Delta TD^3}{\nu^2}. \tag{6}$$

The equations were normalized by using the following dimensionless variables:

$$r = \frac{R}{D} \quad \psi' = \frac{\psi}{\nu} \quad \omega' = \frac{D^2\omega}{\nu}$$

$$\tau = \frac{\nu t}{D^2} \quad \phi = \frac{T - T_\infty}{T_w - T_\infty}.$$

The problem is assumed to be symmetric about the vertical plane passing through the center of the

cylinder and, as a result, only half of the flow domain will be considered in this analysis.

The boundary conditions are:

on the isothermal cylinder surface

$$u' = v' = \psi' = 0 \quad \omega' = -\frac{\partial^2 \psi'}{\partial r^2} \quad \phi = 1; \tag{7}$$

on the symmetry lines

$$v' = \psi' = \omega' = \frac{\partial \phi}{\partial \theta} = 0. \tag{8}$$

Following Kuehn and Goldstein [7], the boundary condition at the far boundary is set as:

at the flow region

$$v' = \frac{\partial^2 \psi'}{\partial r^2} = \phi = 0 \quad \omega' = -\frac{1}{r^2}\frac{\partial^2 \psi'}{\partial \theta^2}; \tag{9}$$

at the outflow region

$$v' = \frac{\partial^2 \psi'}{\partial r^2} = \frac{\partial \phi}{\partial r} = 0 \quad \omega' = -\frac{1}{r^2}\frac{\partial^2 \psi'}{\partial \theta^2}. \tag{10}$$

In addition to the above, boundary conditions must be specified along the baffle. The baffle is assumed to be very thin and to be made of a low thermal conductivity material. It can be easily shown (with a one-dimensional analysis) that a thin, low thermal conductivity baffle exhibits an extremely low fin effectiveness. In addition, the distance from the attaching surface at which the baffle becomes ineffective as a fin is very small. As a result, the heat conduction along the baffle is neglected. Moreover, it is argued that the baffle interferes only with the fluid flow and that there is no temperature difference across the thickness of the baffle. Based on these assumptions, the boundary conditions along the baffle are set as follows:

$$u' = v' = \psi' = 0 \quad \omega' = -\frac{1}{r^2}\frac{\partial^2 \psi'}{\partial \theta^2} \quad \phi = \frac{\phi^+ + \phi^-}{2}, \tag{11}$$

where ϕ^+ and ϕ^- represent the temperature of the fluid a small distance above and below the baffle, respectively.

NUMERICAL SOLUTION

The solution to equations (1)–(3) subject to the boundary conditions specified by equations (7)–(11) was obtained numerically using finite differences. Central differences were used to approximate the diffusive terms, whereas the hybrid scheme was introduced with the convective terms, Patankar [14]. The vorticity along the solid walls was calculated using the following first-order accurate expression:

$$\omega'_w = -\frac{2\psi'_*}{\Delta n^2}, \tag{12}$$

where ψ'_* is the stream function at a short distance Δn into the fluid. A second-order accurate expression was used to evaluate the temperature boundary condition along the symmetry lines. The position of the outer boundary was set in the range $2D \leqslant L \leqslant 3D$ depending on the Rayleigh number. Following Kuehn and Goldstein [7], the change of the far boundary condition from inflow to outflow is set near $\theta = 150°$.

The baffle was discretized as a single row of grid points and, as a result, the voriticity on it takes different values depending on which side of the fluid flow is being considered. The vorticity along the two sides of the baffle was evaluated using an expression similar to equation (12). The temperature along the baffle was set equal to the average temperature of the fluid adjacent to the baffle, as shown in equation (11). The local Nusselt number was calculated using a three-point approximation for the temperature gradient. The average Nusselt number was calculated using the trapezoidal rule.

The majority of the calculations were made using a 90×90 uniform grid mesh. In some cases, however, a much finer grid mesh of 150×90 ($r \times \theta$) was used. For low Ra values, the steady-state solutions were obtained by solving the elliptic form of the governing equations. However, as Ra increased to 10^6, it became difficult to obtain steady-state solutions from the elliptic form of the governing equations when baffles were introduced. In certain cases, the steady-state solutions were obtained by integrating the parabolic form of the governing equations over time. In other cases, the calculations indicate an oscillatory fluid flow behavior near some baffles located at the top portion of the cylinder and thus, no steady-state solution exists to report. All computations were carried out on a 486 personal computer. The resulting algebraic equations were solved using the strongly implicit procedure (SIP), [15].

To ensure that the numerical code is validated, the results were compared with published results for natural convection flow about a horizontal isothermal cylinder. As shown in Table 1, the results obtained with the present code are in good agreement with the solutions presented by Kuehn and Goldstein [7] and Saitoh *et al.* [9].

RESULTS AND DISCUSSION

Solutions are obtained over the range $10^3 \leqslant Ra \leqslant 10^6$ for two baffle lengths $\gamma = 0.25$ and 0.5 and $N = 0, 1, 3, 5, 11$, where N represents the number of equally spaced baffles on each side of the cylinder with no baffle ever attached along the vertical symmetry lines. All results were generated assuming that the fluid is air with $Pr = 0.7$.

The flow and temperature fields corresponding to $Ra = 10^4$ for a cylinder with one baffle of dimensionless length $\gamma = 0.25$ and 0.5 are shown in Fig. 2. The corresponding fields for a cylinder with no baffle

Table 1. Comparison of the present solutions with the results of Saitoh *et al.* [9] and Kuehn and Goldstein [7] for $Ra = 10^3$, 10^4 and 10^5

		Nu							
	Ra	$\theta = 0^\circ$	30°	60°	90°	120°	150°	180°	$\overline{Nu}$
10^3	Present study	3.728	3.692	3.570	3.326	2.847	1.972	1.215	2.967
	Saitoh *et al.* [9]	3.813	3.772	3.640	3.374	2.866	1.975	1.218	3.024
	Kuehn and Goldstein [7]	3.89	3.85	3.72	3.45	2.93	2.01	1.22	3.09
10^4	Present study	5.947	5.887	5.696	5.356	4.726	3.297	1.533	4.788
	Saitoh *et al.* [9]	5.995	5.935	5.750	5.410	4.764	3.308	1.534	4.826
	Kuehn and Goldstein [7]	6.24	6.19	6.01	5.64	4.82	3.14	1.46	4.94
10^5	Present study	10.152	10.025	9.623	8.978	7.973	5.641	1.952	8.065
	Saitoh *et al.* [9]	9.675	9.557	9.278	8.765	7.946	5.891	1.987	7.898
	Kuehn and Goldstein [7]	10.15	10.03	9.65	9.02	7.91	5.29	1.72	8.00

are also included for comparison. Clearly, the presence of one baffle at $\theta = 90^\circ$ forces the ascending hot fluid to travel around it, thus altering the hydrodynamic and thermal characteristics of the problem. Based on the maximum values for ψ', the overall strength of the fluid circulation is reduced slightly with the introduction of the baffle. This weakening of the fluid flow strength is fundamentally due to the additional resistance that the baffle imposes on the fluid flow.

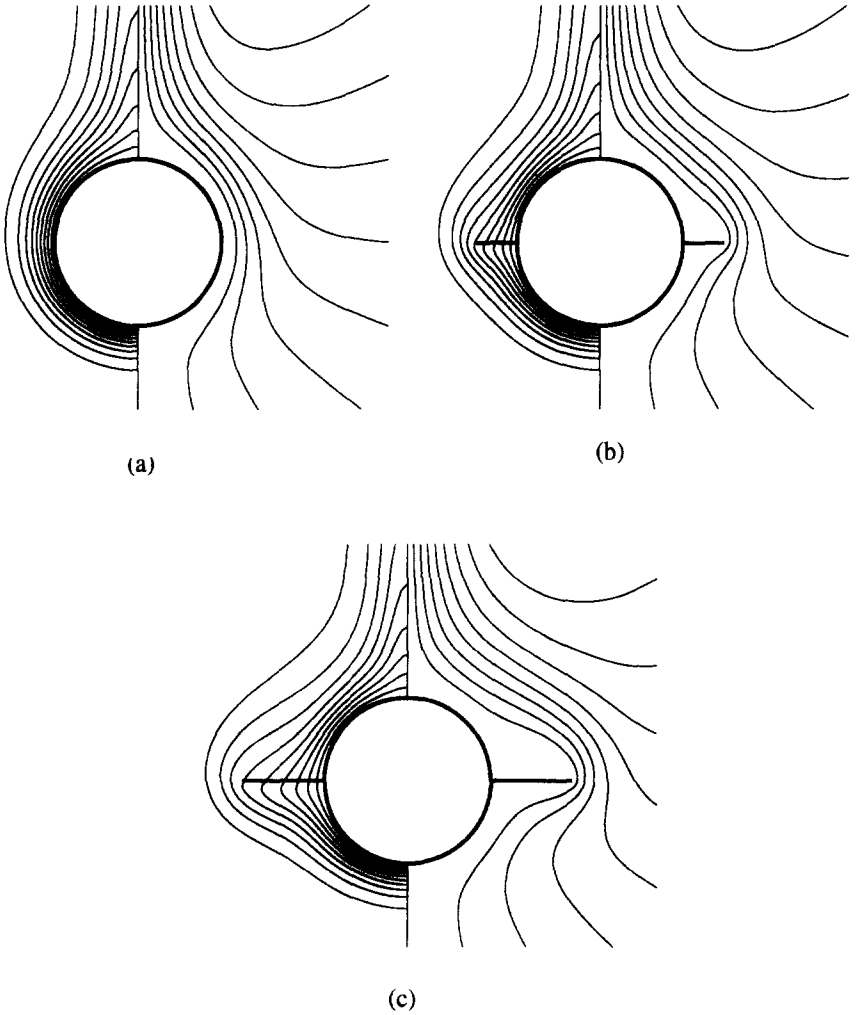

Fig. 2. Uniformly spaced isotherms (LHS) and streamlines (RHS) corresponding to $Ra = 10^4$ ($\Delta\phi = 0.1$ and $\Delta\psi' = 4.0$); (a) $\gamma = 0$, $\psi'_{max} = -42.21$ (b) $\gamma = 0.25$, $\psi'_{max} = -41.45$ (c) $\gamma = 0.5$, $\psi'_{max} = -41.44$.

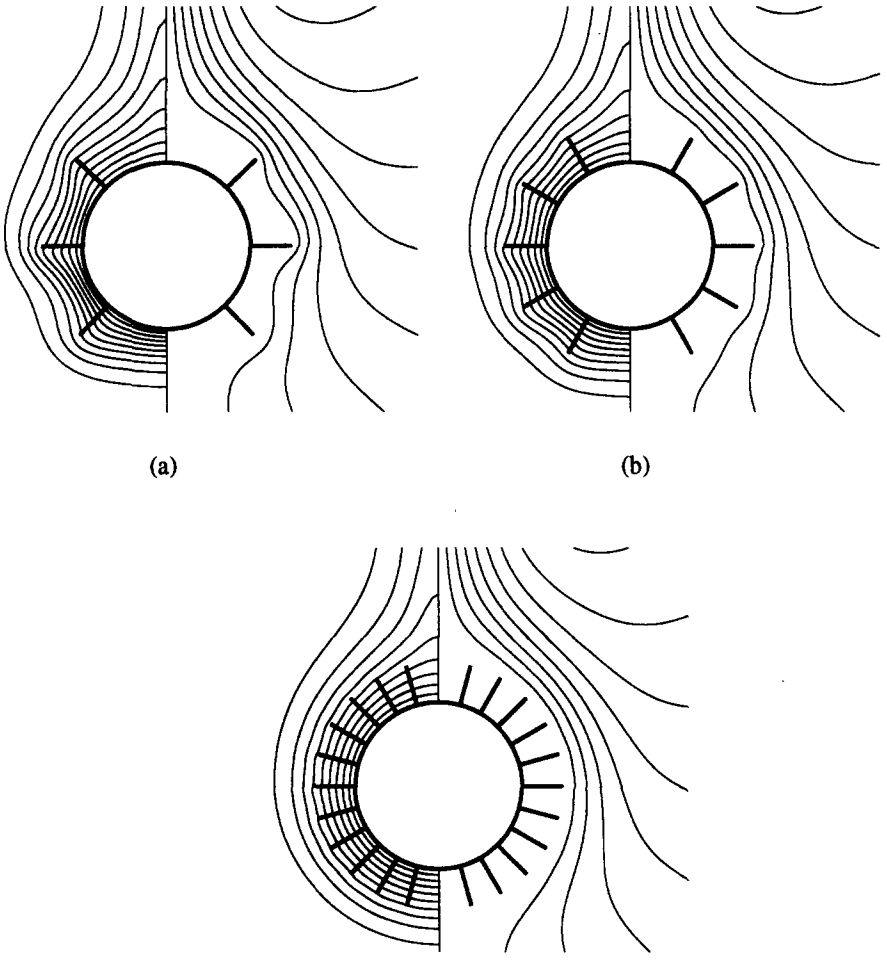

Fig. 3. Uniformly spaced isotherms (LHS) and streamlines (RHS) corresponding to $Ra = 10^4$ ($\Delta\phi = 0.1$ and $\Delta\psi' = 4.0$, $\gamma = 0.25$); (a) 3 equally spaced baffles, $\psi'_{max} = -38.95$; (b) 5 equally spaced baffles, $\psi'_{max} = -38.08$; (c) 11 equally spaced baffles, $\psi'_{max} = -37.76$.

Comparing the two cases, it is obvious that in the case of a cylinder with a baffle the overall hydrodynamic and thermal boundary layer thickness are larger than in the case of a cylinder with no baffle; which, in turn, implies that the heat transfer from the cylinder will be smaller when a baffle is attached. Moreover, the plots indicate that the impact of a baffle on the heat transfer becomes more profound as the baffle length increases.

Figure 3 illustrates the effect on the fluid flow in terms of isotherm and streamline plots when a number of baffles of length $\gamma = 0.25$ are attached on the surface of the cylinder, $Ra = 10^4$. Clearly, as the number of baffles, N, increases, the hot fluid ascends around the baffles in such a way that makes it appear as if another virtual surface (concentric to the cylinder surface) is present at the tip of the baffles, which prevents the fluid from coming close to the surface of the cylinder. The isotherm plots illustrate that the heat loss from the cylinder decreases as the number of baffles increases. Furthermore, at high N values, the isotherms appear as concentric circles, which implies that conduction is the dominant mechanism of heat transfer. Details of the fluid flow structure near the baffles are shown in Fig. 4 for a number of different cases and $Ra = 10^4$. As shown, secondary flows develop downstream of the baffles that are located at the top half portion of the cylinder. These secondary flows grow in strength with increasing baffle length and Ra values and eventually cause the fluid flow structure to become unstable and time dependent.

Local Nusselt number distributions as a function θ are shown for $Ra = 10^4$ and 10^5 in Figs. 5 and 6, respectively. The first number in the labels of Figs. 5 and 6 represents the number of baffles, whereas the second number gives the dimensionless length for the baffles. Clearly, the presence of one baffle at $\theta = 90°$ causes a large reduction in heat transfer along the lower half of the cylinder surface and a slight increase along the top half surface of the cylinder with a large

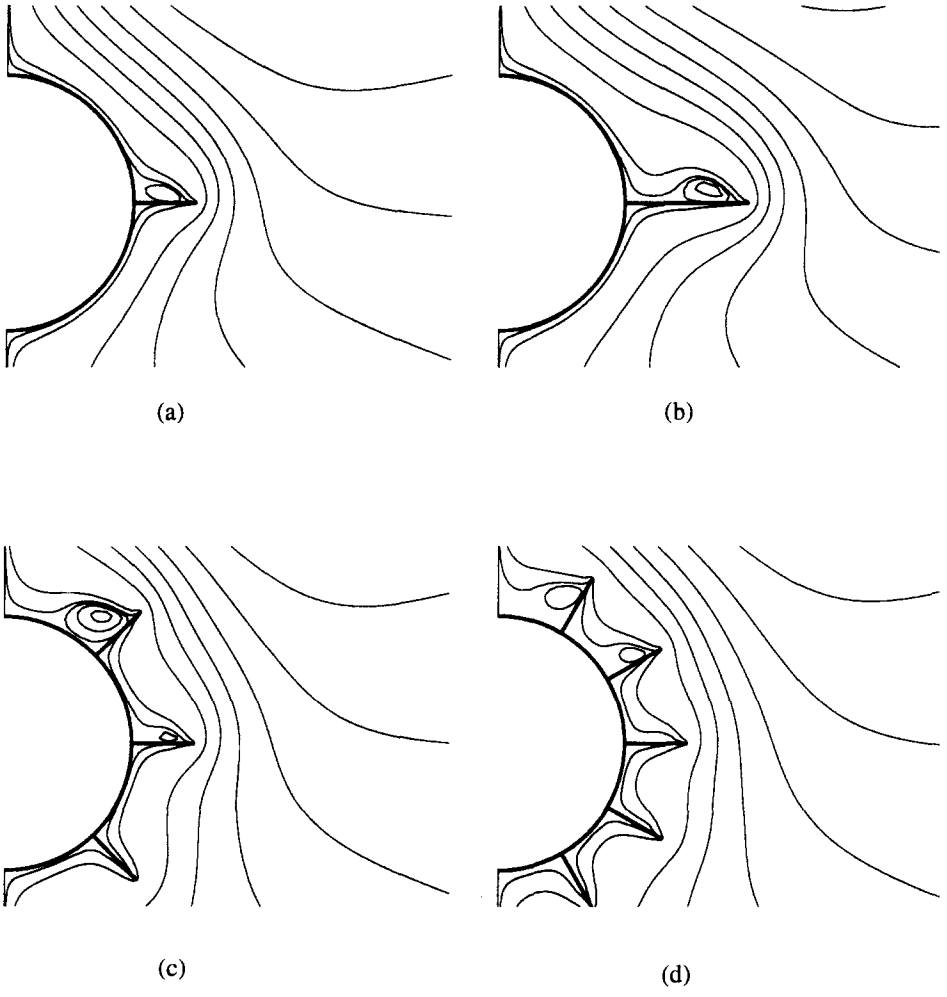

Fig. 4. Detail streamline plot near baffle region corresponding to $Ra = 10^4$; (a) $\gamma = 0.25$; (b) $\gamma = 0.50$; (c) $\gamma = 0.25$; (d) $\gamma = 0.25$.

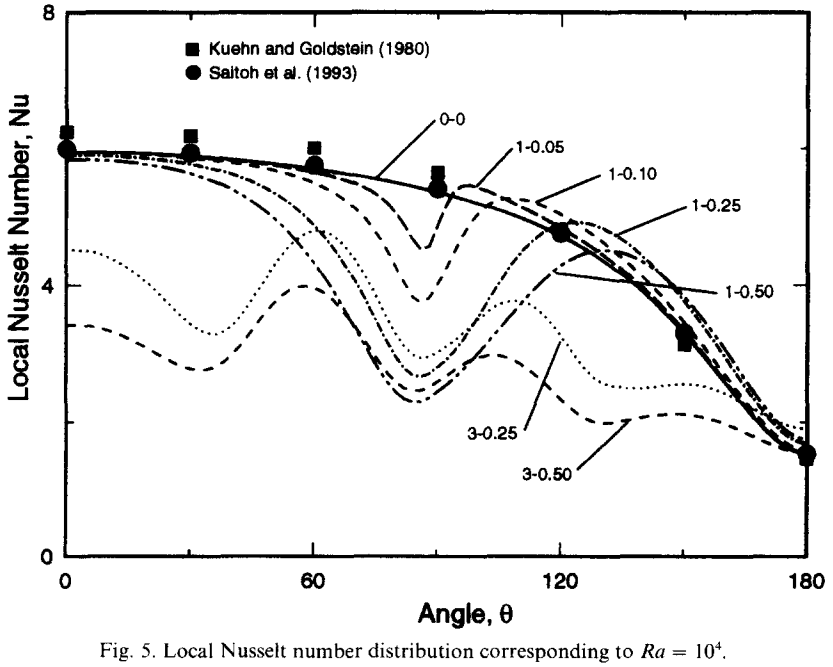

Fig. 5. Local Nusselt number distribution corresponding to $Ra = 10^4$.

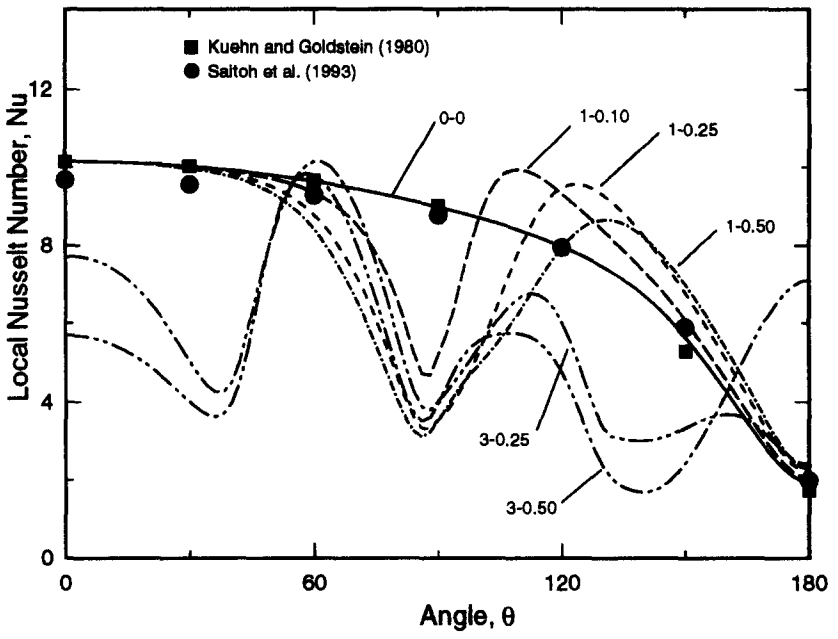

Fig. 6. Local Nusselt number distribution corresponding to $Ra = 10^5$.

variation near the baffle. As expected, the local Nusselt number distribution near the bottom stagnation point is almost not affected when one baffle is used and $\gamma \leqslant 0.1$.

As the number of equally spaced baffles increases to three, the local Nusselt number experiences an overall large decrease with significant variations near each baffle. Although the local Nusselt number distributions corresponding to $Ra = 10^4$ and 10^5 are qualitatively similar, significant differences appear to exist near $\theta = 180°$ for the corresponding cases of $N = 3$ and $\gamma = 0.5$. The increase in the local Nusselt number near $\theta = 180°$ for $Ra = 10^5$ is due to a stronger secondary fluid flow behind the baffle located near the top of the cylinder.

Results in terms of the average Nusselt number are given in Table 2 as a function of Ra, baffle length γ, and number of equally spaced baffles N. Moreover, the reduction in $\overline{Nu}$ relative to the case with no-baffle is calculated and is also given in Table 2. It is clearly observed that the baffles are very effective in reducing the overall heat loss from an uninsulated horizontal cylinder suspended in air. For example, at $Ra = 10^5$, the average Nusselt number can be reduced by 30.8% by attaching six baffles ($N = 3$) of length $0.25D$ to the cylinder as shown in Fig. 1.

As it was stated earlier, the overall heat loss from a cylinder decreases as the number and length of baffles increases. Furthermore, as N increases, the Ra value at which the maximum reduction in $\overline{Nu}$ occurs also increases. An explanation for the existence of an optimum for the reduction in $\overline{Nu}$ is given now. The overall heat transfer loss from a cylinder consists of both conduction and convection. For small Ra values, the

Table 2. Average Nusselt number as a function of Ra, baffle length γ, and number of equally spaced baffles N

			N			
Ra	γ	No-baffle	1	3	5	11
10^3	0.25	2.967	2.676(9.8%)†	2.303(22.4%)	2.203(25.7%)	2.141(27.8%)
	0.50	2.967	2.433(18.0%)	1.863(37.2%)	1.769(40.4%)	1.721(42.0%)
10^4	0.25	4.788	4.330(9.6%)	3.382(29.4%)	3.032(36.7%)	2.819(41.1%)
	0.50	4.788	4.052(15.4%)	2.716(43.3%)	2.274(52.5%)	2.095(56.2%)
10^5	0.25	8.065	7.509(6.9%)	5.579(30.8%)	4.655(42.3%)	3.668(54.5%)
	0.50	8.065	7.221(10.5%)	5.150(36.1%)	4.388(45.6%)	2.549(68.4%)
10^6	0.25	13.724	13.177(4.0%)	‡	‡	7.130(48.0%)
	0.50	13.724	13.004(5.2%)	‡	‡	6.072(55.8%)

† Numbers in parentheses represent % reduction in Nu relative to the corresponding case with no-baffle.
‡ Did not converge to a steady-state solution.

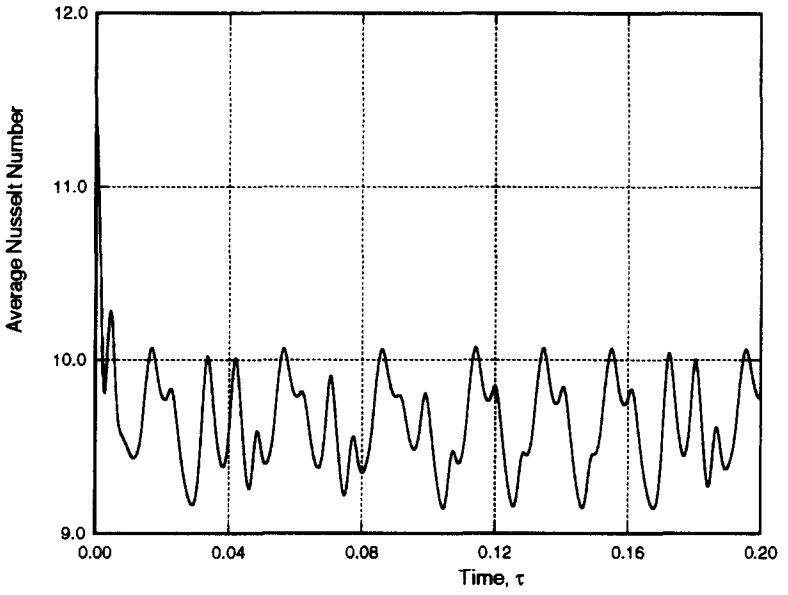

Fig. 7. Average Nusselt number as a function of time corresponding to $Ra = 10^6$, $N = 5$, $\gamma = 0.25$.

heat losses are dominated by conduction. However, as Ra attains large values, convection becomes the dominant mechanism for heat transfer. The baffles affect only the convection heat loss. As stated earlier, the baffles cause the hydrodynamic as well as the thermal boundary layer to thicken which, in turn, implies lower convection losses. As a result, for every baffle configuration, there exists an Ra value for which the reduction in heat loss ($\overline{Nu}$) is maximized. It is interesting to note that in the case of $N = 1$, the percent reduction in $\overline{Nu}$ decreases as Ra increases. Based on the cases considered in this study, the reduction in $\overline{Nu}$ can be as large as 68.4% (see $Ra = 10^5$, $N = 11$, $\gamma = 0.5$).

At $Ra = 10^6$, $N = 5$, and $\gamma = 0.25$, the flow and temperature field became unstable and time dependent. For this case, a transient analysis was performed using an extremely small time step ($\Delta\tau = 10^{-5}$) and a grid mesh of 150×90 ($r \times \theta$). The variation of the average Nusselt number with time corresponding to this case is shown in Fig. 7. It is important to note that the average Nusselt number is still less at all times than the corresponding case with no-baffles. The variation of the flow and temperature fields with time is illustrated in Fig. 8. It is interesting to observe that the instability is mainly localized at the top portion of the cylinder, downstream of the top-most baffle. The flow field near the other four baffles is basically stable and independent of time.

As discussed earlier, the energy savings that are realized when baffles are attached to the cylinder are so large that it is worth examining the potential of using baffles as a way of replacing traditional pipe insulation. As an example, consider a 3 cm diameter pipe which is suspended in air and assume that the temperature difference between the pipe and the ambient air is 60°C. If the air properties are evaluated at 55 C, the corresponding Rayleigh number is $Ra \sim 10^5$. Thus, the heat transfer from an uninsulated horizontal cylinder suspended in air is $\dot{q} \sim 43$ W m^{-1}. Assume now that the pipe is insulated with a 1.5 cm thick material that has a thermal conductivity ratio $k_{ins}/k_{air} = 2$. Using a one-dimensional model together with the correlation given for natural convection over a cylinder by Morgan [1], the heat loss from the insulated pipe is estimated to be equal to 19 W m^{-1}. Consider now the case where baffles are attached to an uninsulated pipe. Clearly, if 22 baffles ($N = 11$) are attached to the cylinder with a length of 0.75 cm ($l/D = 0.25$), the heat loss from the pipe would be approximately 19.6 W m^{-1}. Clearly, the use of this baffle yields a heat transfer rate which is slightly higher than the heat transfer rate achieved with the conventional insulation. On the other hand, if the length of the baffle was increased to 1.5 cm ($l/D = 0.5$), energy savings of about 28.4% would be realized as compared to the insulated case.

It is important to note here that the radiative heat transfer from the surface of the cylinder and the baffles would have to be taken into consideration if baffles were to replace conventional insulation. Usually, an aluminum or steel jacket is used to cover the insulation for the majority of steam pipes used in industrial applications. Both of these materials exhibit low emissivity if it is assumed that they are clean or lightly oxidized. As a result, the radiative heat transfer from the outer surface of the insulation can be neglected. In order to neglect the radiation from the cylinder when only baffles are used, it would require that the emissivity of the cylinder surface be relatively low. Hence, some type of low emissivity jacket would still have to be used to cover the pipe either before attaching the baffles or as part of the baffle attaching mechanism. Furthermore, since the radiative heat loss from the

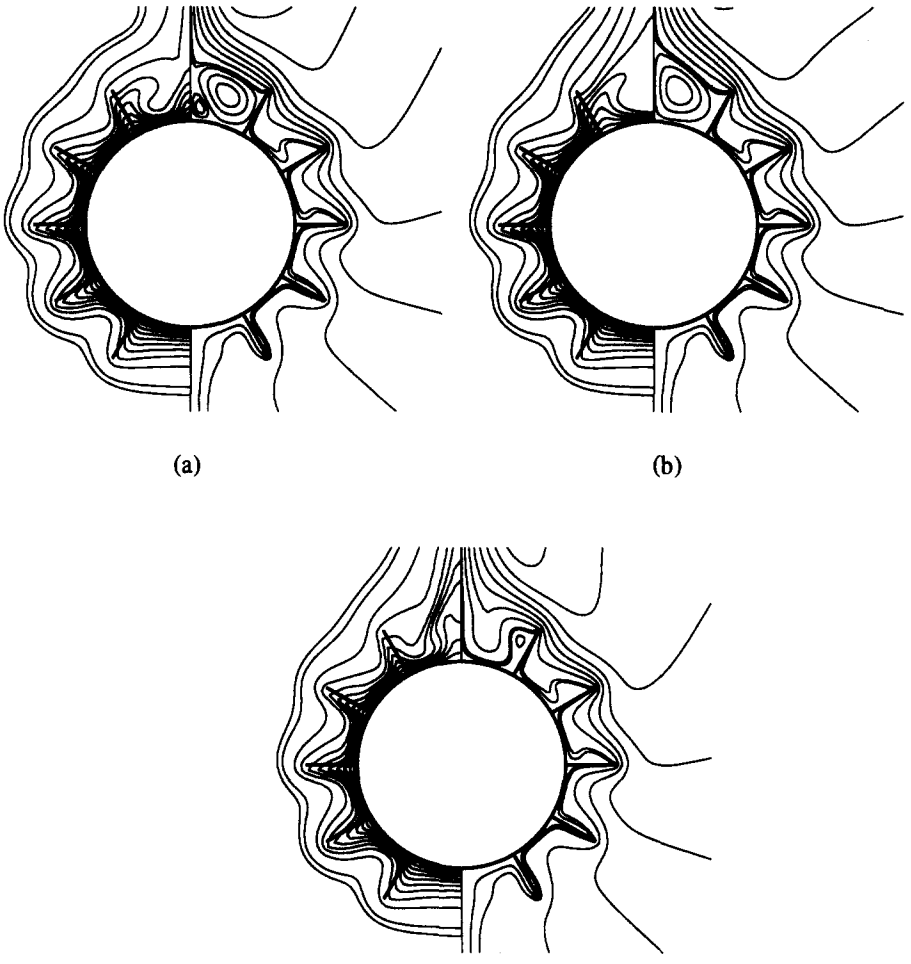

Fig. 8. Isotherms (LHS) and streamlines (RHS) corresponding to $Ra = 10^6$, $N = 5$, $\gamma = 0.25$; (a) $\tau = 0.080$; (b) $\tau = 0.089$; (c) $\tau = 0.097$.

baffle has not been considered in this analysis, it is important to note here that the overall effectiveness of the baffle may be reduced significantly if the loss by radiation is included.

As a final note, it may be that the best way to insulate a pipe is to use an insulation system which is an optimal combination of conventional insulation and longitudinal baffles.

CONCLUSION

The problem of laminar natural convection over an isothermal horizontal cylinder with multiple, low-conductivity, longitudinal baffles has been considered. Results have been obtained over a wide Rayleigh number range of a number of baffle configurations and for two baffle lengths. The overall baffle effectiveness in terms of increasing the thermal resistance to heat flow from the cylinder increases as the number of baffles and the length of the baffles increases. The potential of using baffles as a way of replacing conventional pipe insulation has been examined and discussed. At high Rayleigh numbers the flow field becomes unstable and time dependent. In all cases the average heat loss from the cylinder is still less when baffles are used.

REFERENCES

1. V. T. Morgan, The overall convective heat transfer from smooth circular cylinders, *Adv. Heat Transfer* **11**, 199–264 (1975).
2. R. Hermann, Heat transfer for free convection from horizontal cylinders in diatomic gases, NACA TM 1366 (1954).
3. S. Levy, Integral methods in natural convection flow, *J. Appl. Mech.* **22**, 515–522 (1955).
4. T. Chiang and J. Kaye, On laminar free convection from a horizontal cylinder, *Proceedings of the Fourth National Congress of Applied Mechanics*, pp. 1213–1219 (1962).
5. W. H. McAdams, *Heat Transmission* (3rd Edn), p. 176. McGraw-Hill, New York (1954).
6. S. W. Churchill and H. H. S. Chu, Correlating equations for laminar and turbulent free convection from a horizontal cylinder, *Int. J. Heat Mass Transfer* **18**, 1049–1053 (1975).

7. T. H. Kuehn and R. J. Goldstein, Numerical solutions to the Navier–Stokes equations for laminar natural convection about a horizontal isothermal circular cylinder, *Int. J. Heat Mass Transfer* **23,** 971–979 (1980).
8. B. Farouk and S. I. Guceri, Natural convection from a horizontal cylinder—laminar regime, *ASME J. Heat Transfer* **103,** 522–527 (1981).
9. T. Saitoh, J. Sajiki and K. Maruhara, Bench mark solutions to natural convection heat transfer problem around a horizontal circular cylinder, *Int. J. Heat Mass Transfer* **36,** 1251–1259 (1993).
10. E. M. Sparrow and S. S. Kang, Two-dimensional heat transfer and critical radius results for natural convection about an insulated horizontal cylinder, *Int. J. Heat Mass Transfer* **28,** 2049–2060 (1985).
11. J. O. Jaber, R. F. Babus'Haq and S. D. Probert, Optimal location of a district-heating pipeline within a rectangular duct. *Appl. Energy* **40,** 101–109 (1991).
12. A. J. Neale, R. F. Babus'haq and S. D. Probert, Steady-state heat transfers across an obstructed air-filled rectangular cavity, *Chem. Engng Res. Des.* **66,** 458–462 (1988).
13. J. O. Jaber, R. F. Babus'Haq and S. D. Probert, Optimal thermal-insulation placement of district-heating pipes and their support baffles in air-filled trenches, *Appl. Energy* **40,** 111–118 (1991).
14. S. V. Patankar, *Numerical Heat Transfer and Fluid Flow*, p. 88, McGraw-Hill, New York (1980).
15. H. Stone, Iterative solution of implicit approximations of multidimensional partial differential equations, *SIAM J. Numer. Anal.* **5,** 530–558 (1968).